Mismatch management for optical and matter-wave quadratic solitons

R. Driben, Y. Oz, B. A. Malomed, and A. Gubeskys
Department of Interdisciplinary Studies, School of Electrical Engineering, Faculty of Engineering, Tel Aviv University, Tel Aviv 69978, Israel

V. A. Yurovsky
School of Chemistry, Faculty of Exact Sciences, Tel Aviv University, Tel Aviv 69978, Israel
(Received 22 October 2006; published 23 February 2007)

We propose a way to control solitons in $\chi^{(2)}$ (quadratically nonlinear) systems by means of periodic modulation imposed on the phase-mismatch parameter ("mismatch management," MM). It may be realized in the cotransmission of fundamental-frequency (FF) and second-harmonic (SH) waves in a planar optical waveguide via a long-period modulation of the usual quasi-phase-matching pattern of ferroelectric domains. In an altogether different physical setting, the MM may also be implemented by dint of the Feshbach resonance in a harmonically modulated magnetic field in a hybrid atomic-molecular Bose-Einstein condensate (BEC), with the atomic and molecular mean fields (MFs) playing the roles of the FF and SH, respectively. Accordingly, the problem is analyzed in two different ways. First, in the optical model, we identify stability regions for spatial solitons in the MM system, in terms of the MM amplitude and period, using the MF equations for spatially inhomogeneous configurations. In particular, an instability enclave is found inside the stability area. The robustness of the solitons is also tested against variation of the shape of the input pulse, and a threshold for the formation of stable solitons is found in terms of the power. Interactions between stable solitons are virtually unaffected by the MM. The second method (*parametric approximation*), going beyond the MF description, is developed for spatially homogeneous states in the BEC model. It demonstrates that the MF description is valid for large modulation periods, while, at smaller periods, non-MF components acquire gain, which implies destruction of the MF under the action of the high-frequency MM.

DOI: 10.1103/PhysRevE.75.026612 PACS number(s): 42.65.Tg, 03.75.Lm, 05.45.Yv

I. INTRODUCTION

Solitons are robust localized pulses that have been predicted theoretically and created experimentally in diverse physical settings. The current research in this field is heavily focused on nonlinear optics [1] and Bose-Einstein condensation (BEC) [2]. Typical solitons are found in uniform media with constant characteristics. However, in many cases it is necessary to consider solitary waves (which are also called "solitons," in a loose sense, even if they are not described by integrable equations) traveling across heterogeneous media, or subjected to strong time modulation. A well-known example of the former setting is *dispersion management*, which is an important concept in fiber-optic telecommunications, helping to support stable soliton trains used as data-carrying streams [3,4]. On the other hand, a possibility to stabilize matter-wave solitons by means of the *nonlinearity management*, applied to them via the Feshbach resonance in a time-modulated magnetic field (i.e., time-periodic variation of the scattering length that determines the coefficient in front of the cubic term in the Gross-Pitaevskii equation), in 1D (one-dimensional) [5] and 2D (two-dimensional) [6] geometries, has drawn considerable attention in the studies of BEC. Another example of a setting supporting the transmission of robust solitons in a strongly heterogeneous periodic system, that combines features of both the dispersion management and nonlinearity management, is the *split-step model* (SSM). In the simplest case, it is composed of periodically alternating pieces of optical fibers with zero dispersion and zero nonlinearity (i.e., it is built as a periodic concatenation of nonlinear and dispersive segments, the latter ones taken with anomalous dispersion) [4,7]. In a more general variant of the SSM, the nonlinear and dispersive segments are allowed to have nonvanishing dispersion and nonlinearity, respectively [8]. Multicomponent generalizations of the SSM were elaborated too, including one for the WDM (wavelength-division-multiplexed) system [9], and a model taking into regard two polarizations of light and the polarization-mode dispersion [10].

In the above-mentioned examples, solitons are supported by the cubic nonlinearity of the medium. It is well known that the quadratic (second-harmonic-generating, alias $\chi^{(2)}$) nonlinearity also gives rise to stable solitons, that have been studied in detail theoretically and experimentally in optics [11]. In most cases, these are *spatial solitons*, i.e., self-supporting localized beams in bulk or planar waveguides. Temporal $\chi^{(2)}$ solitons have been created too [11,13], but under very sophisticated conditions.

In terms of BEC, a counterpart of the second-harmonic generation is the Feshbach association in atomic BEC [14–16], induced by the coupling of atomic and molecular mean fields (MFs) with the help of resonant optical fields or by hyperfine interactions, using the Zeeman effect for the mismatch tuning. Quasi-1D BEC can be realized in atomic waveguides, which tightly confine the atomic and molecular motion in two directions, leaving it free in the third, axial, direction. Quadratic solitons in BEC have been predicted in Ref. [17]. For the comparison with optics, these solitons in BEC may be classified as temporal ones.

In those studies, it was established that conditions for the existence and stability of $\chi^{(2)}$ solitons are most sensitive to the mismatch between the fundamental-frequency (FF) wave

and the second harmonic (SH), or, in terms of the BEC, between the atomic and molecular MFs. This fact suggests a natural question, which is the subject of the present paper—how the quadratic solitons will react to a periodic modulation of the mismatch, i.e., "mismatch management" (MM). The issue is of general interest, as a possible contribution to the theory of the "soliton management" [4], and may also be potentially promising as concerns the use of $\chi^{(2)}$ spatial solitons in optical switching [11] and other applications to photonics. As for the soliton-management schemes, almost all of them were explored in terms of media with the cubic nonlinearity; the only example dealing with a $\chi^{(2)}$ setting was the model of "tandem solitons", which assumed their transmission in a waveguide built as a concatenation of $\chi^{(2)}$ and linear segments, in 1D [18] and 2D [19] geometry (actually, the tandem model was introduced with the purpose of reducing the mismatch).

A ubiquitous approach to the reduction of mismatch in optical waveguides is based on the use of the quasi-phase-matching (QPM) scheme, in which the material of the $\chi^{(2)}$ waveguide is subjected to periodic poling (since the material, such as $LiNbO_3$, is a ferroelectric, this is usually carried out through periodic reversal of the orientation of ferroelectric domains) [20]. The poling gives rise to a change of the sign of the $\chi^{(2)}$ coefficient with a certain period, $L_{\rm QPM}$, and thus adds an extra wave vector, $\mathbf{k}_{\rm QPM}=(2\pi/L_{\rm QPM})\mathbf{e}_z$, aligned with the propagation direction, $\mathbf{e}_z$, to the relation between the FF and SH wave vectors, $\mathbf{k}_{\rm FF}$ and $\mathbf{k}_{\rm SH}$, which may be used to cancel the original mismatch, $2\mathbf{k}_{\rm FF}-\mathbf{k}_{\rm SH}$. In terms of this technique, the MM may be implemented by imposing a long-period supermodulation on the QPM poling.

The MM may also be implemented in the above-mentioned atomic-molecular BEC, through the Feshbach-management technique. As mentioned above, in terms of BEC, the application of the latter technique, which is based on the Feshbach resonance driven by a modulated magnetic field, to the stabilization of various types of 1D [5], 2D [6], and 3D (three-dimensional) [21] matter-wave solitons (as concerns the multidimensional solitons, see also Ref. [22]) was theoretically elaborated for the atomic BEC which obeys the Gross-Pitaevskii equation with the cubic nonlinearity, but no similar results were reported, thus far, for atomic-molecular condensates.

Although at large values of the mismatch a $\chi^{(2)}$ system may be reduced to a $\chi^{(3)}$ limit by means of the well-known cascading approximation (see more details below), there is a fundamental difference between the systems. While $\chi^{(3)}$ models may have exact Bethe-ansatz solutions [23] even beyond the MF approximation, the introduction of the SH (the molecular field) destroys the integrability [24]. Thus, we expect effects of MM in $\chi^{(2)}$ systems, at small or moderate values of the mismatch, to be different from earlier studied effects of the nonlinearity management in the $\chi^{(3)}$ model (in the cascading limit, the $\chi^{(2)}$ MM goes over into the $\chi^{(3)}$ nonlinearity management, as shown below).

The objective of the paper is to study solitons and their stability in one-dimensional MM systems, in both the optical and BEC realizations. The MF model, based on a set of partial differential equations, is introduced in Sec. II. A piecewise-constant periodic modulation of the mismatch parameter in this model is natural in the optical setting. Basic results for solitons in the MF model (in terms of the optical waveguide) are collected in Sec. III (where the cascading approximation is considered too). We report stability regions for the solitons, and conditions necessary for their self-trapping from input beams. Interactions between stable solitons are considered too, with a conclusion that characteristics of the interactions in the MM system are virtually the same as in its ordinary (unmodulated) counterpart.

In Sec. IV, we resort to the parametric approximation (formulated in terms of the atomic-molecular BEC) [25], which goes beyond the mean field, and apply it to spatially uniform configurations. Although this setting does not generate solitons, it allows us to explicitly analyze effects of quantum fluctuations, which may be important in both optical [26] and, especially, BEC [25] realizations of the $\chi^{(2)}$ interactions, as well as relaxation effects, which appear in the BEC due to inelastic collisions. In the framework of this analysis, we adopt, as is usual for BEC, the harmonic form of the periodic modulation of the magnetic field which tunes the Feshbach resonance (rather than the piecewise-constant format, adopted in the optical model). Numerical solutions of parametric-approximation equations demonstrate that the noncondensate (fluctuational) component in the atomic-molecular gas is not essentially excited by the MM, under a natural condition that the modulation frequency is low enough. On the other hand, the modulation at higher frequencies may lead to a quantum instability of the condensate and, eventually, its destruction. The paper is concluded by Sec. V.

II. THE MISMATCH-MANAGEMENT MODEL FOR THE OPTICAL MEDIUM

In a normalized form, which is widely adopted in nonlinear optics, the fundamental $\chi^{(2)}$ model in one dimension is based on a system of coupled equations for complex local amplitudes of the FF and SH waves, $u(z,x)$ and $v(z,x)$ [11],

$$iu_z + u_{xx} - u + vu^* = 0,$$

$$2iv_z + v_{xx} - \alpha v + (1/2)u^2 = 0, \tag{1}$$

where α is the mismatch parameter [this coefficient is an irreducible one in the framework of the notation adopted in Eqs. (1), if solitons are intended to be looked for in the z-independent form], and the asterisk stands for the complex conjugation. Here, it is assumed that, in the case of spatial solitons, light propagates along axis z in a planar waveguide with the transverse coordinate x. In terms of temporal solitons, x is the reduced-time variable. MF equations for atomic-molecular BEC in an atomic waveguide, where x is directed along the waveguide axis, can be reduced to the form of Eq. (1) as well, with z being time (see Sec. IV below).

In the notation of Eq. (1), complete matching is attained at $\alpha=4$, while the single exact analytical solution for the $\chi^{(2)}$ soliton is available at $\alpha=1$,

$$u = \pm(3/\sqrt{2})\mathrm{sech}^2(x/2), \quad v = (3/2)\mathrm{sech}^2(x/2) \tag{2}$$

(the *Karamzin-Sukhorukov* soliton [28]). At other values of

α, solitons were found numerically [11], as well as in an approximate analytical form, by means of the variational method [12].

The simplest model of the MM (similar, in particular, to those of the dispersion management [3,4] and SSM [4,7,8]) assumes periodic modulation of α according to the following *map* (the latter term follows the pattern of the *dispersion-management map* [3,4]):

$$\alpha(z) = \begin{cases} \alpha_0 - \Delta\alpha, & nL < z < (n+1/2)L, \\ \alpha_0 + \Delta\alpha, & (n+1/2)L < z < (n+1)L, \end{cases}, \quad (3)$$

$$n = 0,1,2,3, \ldots,$$

where α_0 is the average value of α, while $\Delta\alpha$ and L are the amplitude and period of the management. We here assume equal lengths, $L/2$, of the two segments forming the MM cell. Simulations demonstrate that a change of the relative length of the two segments (with the respective change of the local values of the mismatch in them) produces little effect on eventual results, quite similar to what is known about the dispersion management [3,4].

While the MM map in the piecewise-constant form of Eq. (3) is most natural in terms of optical waveguides, for the application to the atomic-molecular BEC a more natural choice is, as mentioned above, the harmonic modulation of the mismatch, corresponding to the periodic time dependence of the magnetic field tuning the Feshbach resonance, see Eq. (15) below. The experience gained in the studies of various models of the dispersion management [4] suggests that the piecewise-constant and harmonic formats of the modulation cannot lead to qualitatively different results.

Equations (1) conserve a known integral of motion, the *Manley-Rowe invariant*,

$$I_{\mathrm{MR}} = \int_{-\infty}^{+\infty} [|u(x)|^2 + 4|v(x)|^2]dx, \quad (4)$$

even in the case of the z-dependent mismatch parameter, whereas the Hamiltonian corresponding to Eqs. (1) is not conserved in that case. In addition, Eqs. (1) with variable $\alpha(z)$ conserve the total momentum,

$$P = 2i\int_{-\infty}^{+\infty} (u_x^* u + 2v_x^* v)dx, \quad (5)$$

which is relevant to "walking" solitons [27] [in the present case, these are spatial solitons tilted in the plane of (x,z)]. It is also worthy to note that Eqs. (1) with $\alpha=\alpha(z)$ are invariant with respect to the (spatial) Galilean boost, hence a generic tilted soliton, $(\tilde{u},\tilde{v})$, can be generated from the straight one by means of the corresponding transformation,

$$\tilde{u}(x,z) \equiv e^{i(c^2/4)z+i(c/2)x}u(x-cz),$$

$$\tilde{v}(x,z) \equiv e^{i(c^2/2)z+icx}v(x-cz),$$

with an arbitrary real tilt parameter c. As follows from Eqs. (4) and (5), the momentum of the tilted soliton is $P=cI_{\mathrm{MR}}$, i.e., c and I_{MR} play the role of the effective velocity and mass of the soliton.

In the case of the atomic-molecular BEC, the Galilean invariance has its literal meaning (in the temporal, rather than spatial, domain).

III. DYNAMICS OF SPATIAL SOLITONS UNDER THE MISMATCH MANAGEMENT IN THE OPTICAL MODEL

A. Formation of stable mismatch-managed solitons

To simulate the transmission of spatial optical solitons under the MM conditions, we solved equations (1) with MM map (3) by means of the split-step numerical method, which uses the Fourier transform to handle the linear stage of the evolution. As the input (initial pulse), we took either an ordinary soliton corresponding to the averaged version of the model, i.e., one with $\alpha(z)\equiv\alpha_0$, or a deliberately altered pulse, to verify whether the MM system will provide for self-trapping into a stable transmission regime. Below, we display systematic results obtained for $\alpha_0=1$ and $\alpha_0=2$ (comparison with results collected with other values of the average mismatch parameter demonstrate that these two cases adequately represent the generic situation). In particular, for $\alpha_0=1$ we launched the initial pulse taken as exact solution (2) corresponding to $\alpha=1$. For $\alpha_0=2$, we typically used either a soliton solution found in a numerical form for $\alpha=2$, or, in order to try the effect of a strong change of the input, we again took expression (2), i.e., the exact soliton appertaining to $\alpha=1$. At a fixed value of α_0, results were collected by varying the MM amplitude $\Delta\alpha$ and period L.

First, in Fig. 1 we display a typical numerical solution for $\alpha_0=1$, $L=1$, and $\Delta\alpha=1$, generated with the use of exact soliton (2) as the initial condition. In this figure, panels (a) and (b) present the evolution of the FF and SH components of the field. In fact, in all cases considered, there was no conspicuous difference in the dynamics of the two components, therefore in other cases shown below we only display the picture for the FF beam. As seen from Fig. 1, the input beam readily gives rise to a robust spatial soliton (intrinsic pulsations with period $L=1$, caused by the MM, are almost invisible in Fig. 1); the soliton remains stable in indefinitely long simulations. The transient stage, necessary for the self-trapping, is fairly short, comprising a few MM cells. In the subsequent evolution, gradually fading residual oscillations of the pulse's amplitude can be seen, with a period covering several cells (these oscillations are caused by the initial perturbation, rather than the periodic MM). Further examples of stable transmission regimes are displayed below in Figs. 3(a) and 3(c).

B. Stability diagrams

Conclusions drawn from systematic simulations are summarized in stability diagrams, which are displayed in Fig. 2 for $\alpha_0=1$ (a) and $\alpha_0=2$ (b). As said above, in the former case we launched the pulse corresponding to Karamzin-Sukhorukov soliton (2), which is an exact solution for $\alpha(z)\equiv 1$, and in the latter case the initial pulse was a numerically found stationary soliton corresponding to $\alpha(z)\equiv 2$. The diagrams display areas in parameter plane $(\Delta\alpha,L)$ where the

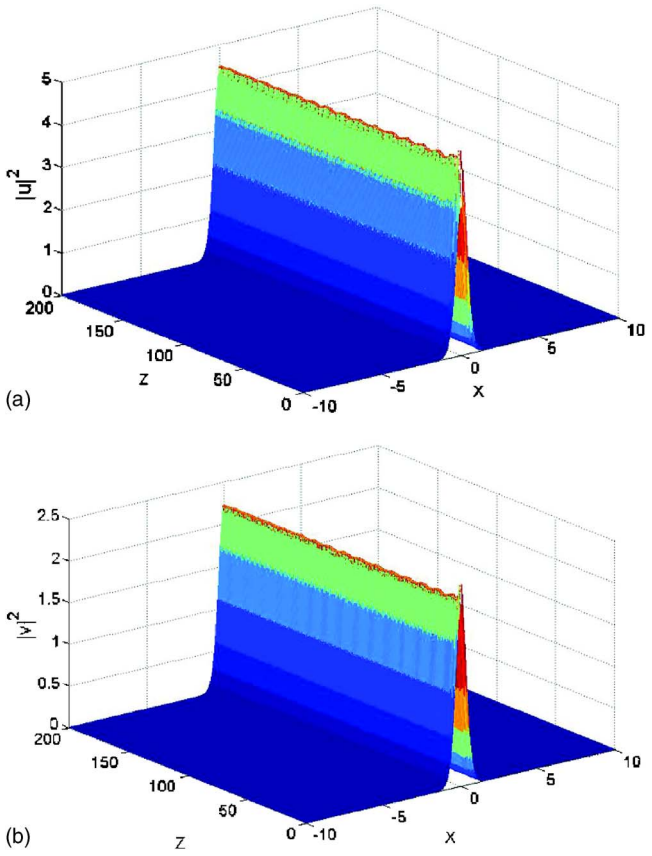

FIG. 1. (Color online) A typical example of the quick self-trapping of an initial beam into a stable spatial soliton in the mismatch-management model, with $\alpha_0=L=\Delta\alpha=1$. The input was the *Karamzin-Sukhorukov* soliton for $\alpha(z)\equiv 1$, taken as per Eq. (2). Panels (a) and (b) show the evolution of the FF and SH fields.

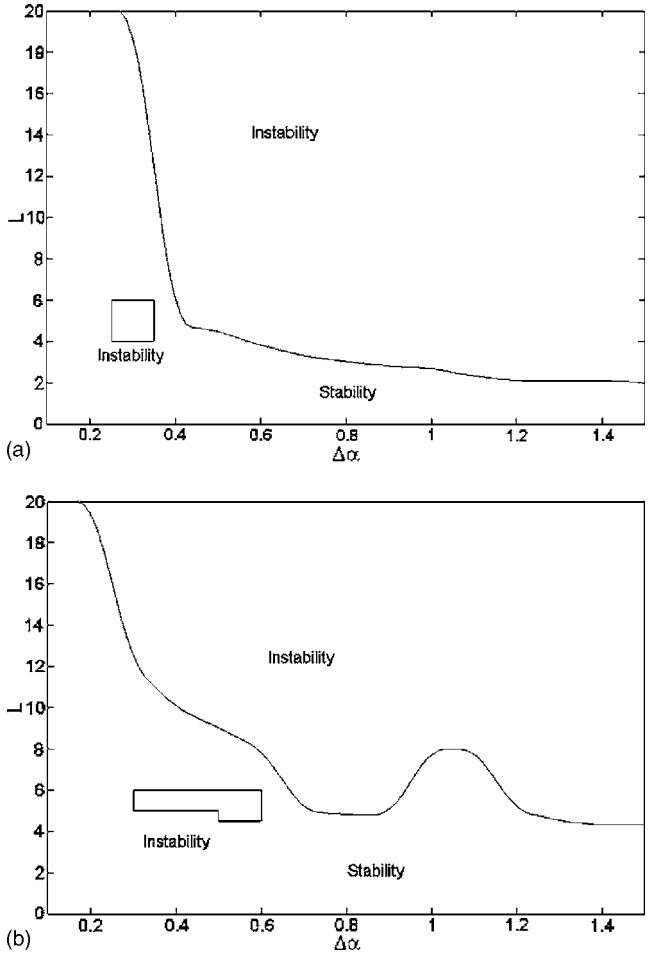

FIG. 2. Stability and instability areas in the mismatch-management model, in the plane of the management amplitude ($\Delta\alpha$) and period (L). Panels (a) and (b) display the stability diagrams for the model with average mismatch $\alpha_0=1$ and $\alpha_0=2$, respectively. In either case, the diagram was built by collecting results of many simulations, with the input taken as a soliton of the respective averaged model, i.e., one with $\alpha(z)\equiv\alpha_0$ [for $\alpha_0=1$, the initial pulse is the analytical Karamzin-Sukhorukov solution, given by Eq. (2)].

initial pulse gives rise to stable transmission, or decay of the pulse [an example of the latter outcome is displayed below in Fig. 3(b)]. Naturally, the stability regions tend to extend along the parameter axes, as, in either limit of $\Delta\alpha\to 0$ or $L\to 0$, the model returns to the usual $\chi^{(2)}$ system (in the case of $L\to 0$, this is provided by averaging), where the initial pulse represents an ordinary stable soliton.

Generally, the instability of the $\chi^{(2)}$ solitons in a part of the parameter space may be realized as a result of a *resonance* between the perturbation frequency, introduced by the periodic action of the MM, and the frequency of the intrinsic mode, which, as is well known, $\chi^{(2)}$ solitons have in the system with constant coefficients [11]. Indeed, comparison of the numerically found instability border, shown in Figs. 2(a) and 2(b), with values of the intrinsic eigenfrequency, which are known from numerical computations too, demonstrates that the explanation of the instability by the resonance is feasible, although the intrinsic frequency is defined for infinitely small perturbations, while the instability sets in when the solitons are strongly perturbed.

At large absolute values of mismatch α, the above-mentioned cascading approximation makes it possible to express the SH amplitude in terms of the FF field, neglecting the first two terms in the second equation in system (1), $v\approx u^2/2\alpha$. Then, the substitution of this in the first equation reduces the $\chi^{(2)}$ system to the single NLS equation,

$$iu_z + u_{xx} - u + (2\alpha(z))^{-1}|u|^2u = 0. \tag{6}$$

Equation (6) features periodic *nonlinearity management* [4]. Solitons in the latter equation and their stability were investigated in some detail in various contexts [4,5]. In particular, a *resonant* mechanism of the destabilization (splitting) of higher-order solitons (bound states of fundamental solitons) under the action of the nonlinearity management, qualitatively similar to one outlined above, has been demonstrated in Ref. [29].

Besides the use of the cascading approximation, another semianalytical approach might be based on the variational approximation (VA). However, unlike this approximation for static $\chi^{(2)}$ solitons in the case of $\alpha=$const [12], the VA for the nonstationary solitons is very messy, involving a system of seven nonautonomous evolution equations for two widths,

two amplitudes, and two chirps of the FF and SH components of the soliton, and their relative phase.

A noteworthy feature of the diagrams is the presence of an *instability enclave* inside the stability area. In Fig. 2(a), the enclave is shown symbolically by a square, as exact delineation of its borders requires extremely long simulations. In Fig. 2(b), the borders of the enclave approximately correspond to its real shape. It may be relevant to mention that examination of similar stability diagrams in the above-mentioned SSM had revealed a different but somewhat similar feature, viz., a system of *stability islands* inside the instability area at large values of L [7]. In the present MM model, the simulations do not reveal stability islands (on the other hand, no "instability lakes," that would be similar to the enclaves in Fig. 2, were found inside the stability area in the SSM). We surmise that there may exist additional small instability enclaves, and, in principle, they may even form a fractal pattern. However, an accurate investigation of these issues requires extremely high numerical accuracy, and they are left beyond the scope of this work.

The existence of the instability enclave is further illustrated by a set of simulations presented in Fig. 3, which are performed along a vertical line, $\Delta\alpha=0.3$, cutting through the enclave in Fig. 2(a). A notable difference is observed in the self-trapping into stable transmission regimes below and above the instability region: in the former case, at $L=4$ (which is close to the instability border), the established pulse is very different from the input, due to considerable radiation loss in the process of the establishment of the stable-transmission regime (in the SH component of the wave field, which is not shown in Fig. 3, an approximately the same degree of the loss is observed). It is relevant to mention that the formation of stable solitons in the SSM may also be accompanied by strong losses, depending on parameters of the system and the form of the input [7]. On the other hand, above the instability enclave, the loss is small, and the established soliton is closer to the input, as seen in Fig. 3(c) (the same is observed in the SH counterpart of the latter figure, which is not shown here).

C. System's tolerance to variations of the input pulse

Another noteworthy feature revealed by the simulations is great tolerance of the spatial solitons established in the MM system to variance of the input beam. In particular, if the input launched into the system with $\alpha_0=2$ was deliberately taken in the "wrong" form of expressions (2) (recall they would yield an exact solution for the averaged equations with $\alpha=1$, rather than $\alpha=2$), the simulations, performed for various values of $\Delta\alpha$ and L, produced a stability diagram nearly identical to that shown in Fig. 2(b).

It is natural to expect that decrease of the input power will eventually lead to a failure in the self-trapping of the spatial soliton, i.e., there must exist a certain power threshold for the soliton formation. To find it, we performed additional simulations with inputs similar to those used above [in particular, wave form (2) was taken for $\alpha_0=1$], but multiplied by a power-reducing factor, $W<1$,

$$\{u_0(x),v_0(x)\} \to \sqrt{W}\{u_0(x),v_0(x)\}. \tag{7}$$

It was found that the critical value of W, below which the thus altered input pulse (2) fails to generate a stable soliton is

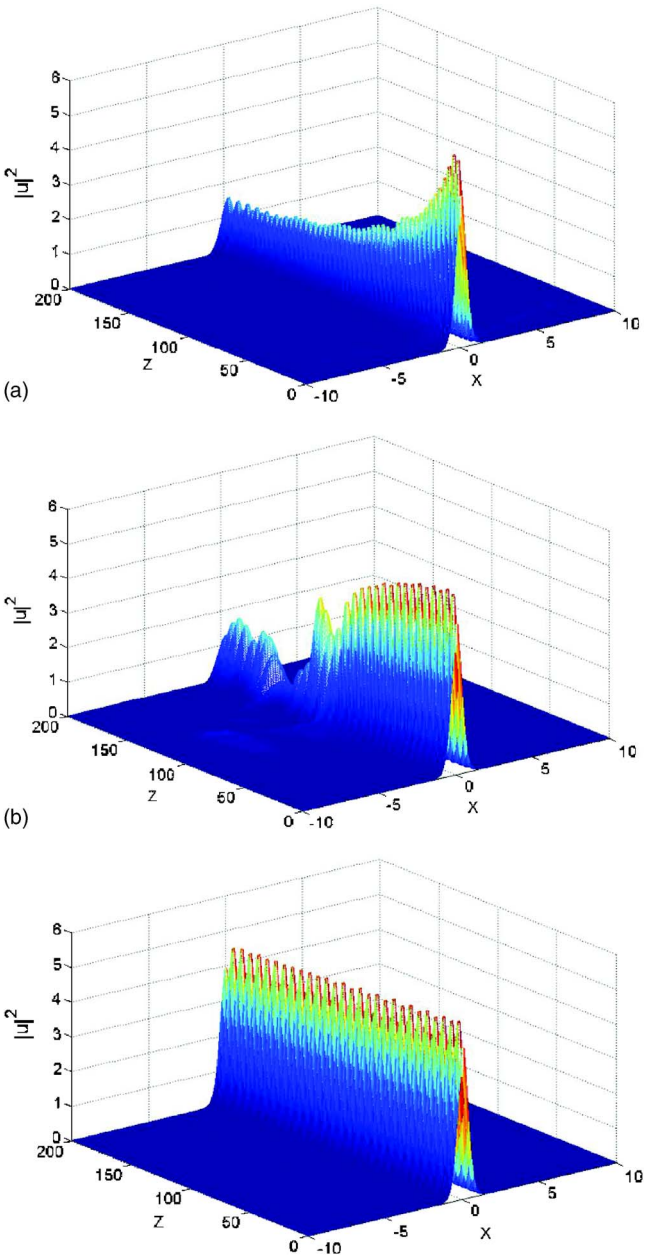

FIG. 3. (Color online) Three examples of the evolution generated by the input in the form of Eq. (2) launched into the mismatch-management system with $\alpha_0=1$ and $\Delta\alpha=0.3$, the modulation period being $L=4$ (a), 6 (b), and 7 (c). Point (b) falls into the instability enclave in Fig. 2(a); in this case, the soliton suffers, eventually, complete destruction.

$W_{\rm cr}\approx 0.72$ (in fact, it is close to a critical value that can be found numerically in the ordinary $\chi^{(2)}$ system, with $\Delta\alpha=0$). Figures 4(a) and 4(b) show what happens when W is taken, respectively, above and below $W_{\rm cr}$.

It was also checked that the change of the distribution of the Manley-Rowe invariant [see Eq. (4)] between the two components of the input beam virtually does not affect the self-trapping threshold (in particular, one may start with the entire power put in the FF field, while $v_0=0$). The ordinary $\chi^{(2)}$ system, with $\Delta\alpha=0$, features a similar property [11].

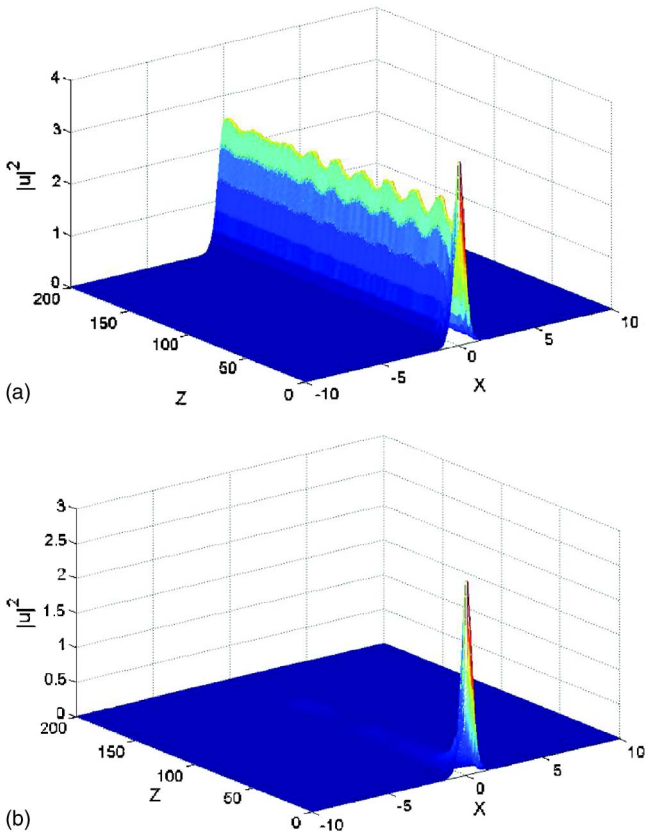

FIG. 4. (Color online) (a) Self-trapping into a stable mismatch-managed spatial soliton of the input taken as per Eq. (7) with $W=0.81$. (b) Decay of the input beam taken as in Eq. (7), but with $W=0.64$. In either case, $u_0(x)$ and $v_0(x)$ are components of soliton solution (2), and parameters are $\alpha_0=\Delta\alpha=L=1$.

D. Soliton-soliton interactions

We have also performed systematic simulations of interactions between solitons in the MM model. It was found that the character of the interaction remains virtually the same as in the ordinary $\chi^{(2)}$ model with constant mismatch, that was studied in detail in earlier works [11]. The main characteristic of the interaction is a minimum initial separation between co-propagating identical in-phase solitons, $\Delta x_{\min}$, which is defined so that the solitons do not demonstrate any interaction for $\Delta x > \Delta x_{\min}$, while, being placed at distance $\Delta x < \Delta x_{\min}$, they start to attract each other and eventually merge into a single beam. A typical example displayed in Fig. 5 shows that the interaction indeed seems almost identical in the MM system and its ordinary counterpart.

IV. EFFECTS OF RELAXATION AND QUANTUM FLUCTUATIONS

As explained in Introduction, the $\chi^{(2)}$ model can also describe a hybrid atom-molecule BEC [14] under quasi-1D confinement. In the parametric approximation, developed for the case of free space in Ref. [25], the condensate is described by the following system of equations of motion for the molecular mean field $\varphi_m(X,t)$ and the atomic annihilation operators $\hat{\Psi}_a(X,t)$,

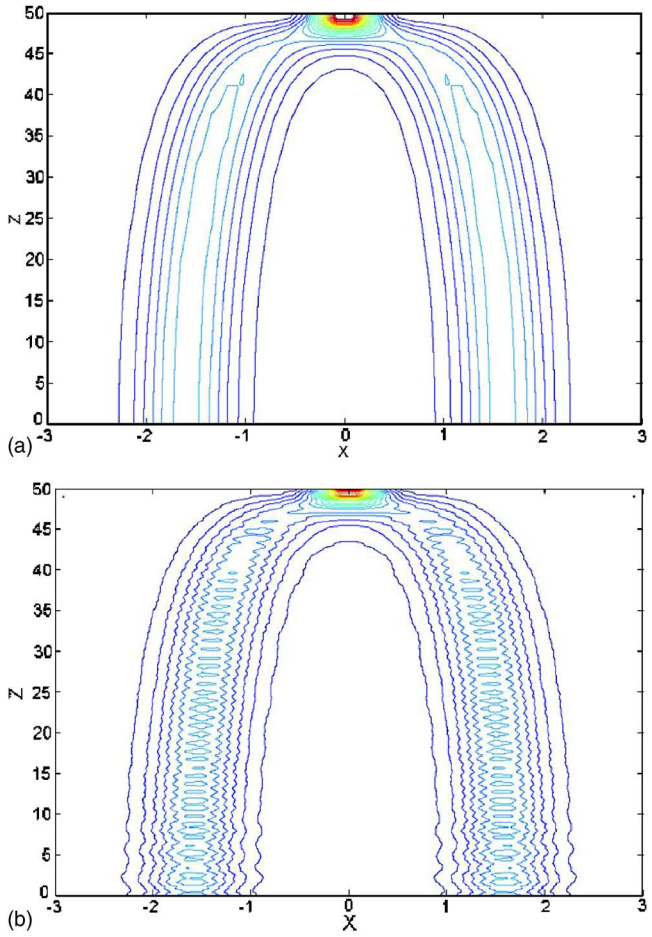

FIG. 5. (Color online) Interaction of two identical in-phase solitons in the ordinary $\chi^{(2)}$ model (with $\alpha=1$, $\Delta\alpha=0$) (a), and its mismatch-managed counterpart with $\alpha_0=\Delta\alpha=L=1$ (b). The initial separation between the solitons is $\Delta x=3.8$, while the minimum separation at which the solitons do not interact is $\Delta x_{\min}\approx 5$, in this case.

$$i\frac{\partial}{dt}\varphi_m(X,t) = -\frac{1}{4m}\frac{\partial^2}{\partial X^2}\varphi_m(X,t) + g\langle\hat{\Psi}_a(X,t)\hat{\Psi}_a(X,t)\rangle - i\left(\frac{k_a}{2}\langle\hat{\Psi}_a^{\dagger}(X,t)\hat{\Psi}_a(X,t)\rangle + k_m|\varphi_m(X,t)|^2\right)\varphi_m(X,t), \tag{8}$$

$$i\frac{\partial}{dt}\hat{\Psi}_a(X,t) = \left(-\frac{1}{2m}\frac{\partial^2}{\partial X^2} - \frac{1}{2}D_{1D}(t)\right)\hat{\Psi}_a(X,t) + 2g^*\varphi_m(X,t)\hat{\Psi}_a^{\dagger}(X,t) - \frac{1}{2}ik_a|\varphi_m(X,t)|^2\hat{\Psi}_a(X,t) + i\hat{F}(X,t), \tag{9}$$

where m is the atomic mass and units with $\hbar=1$ are used. As shown in Ref. [30], the 1D coupling constant, g, and (time-dependent) detuning D_{1D} can be expressed, as follows, in terms of elastic scattering length a_{bg}, phenomenological

Feshbach-resonance strength Δ, the difference between the magnetic momenta of an atomic pair in the open and closed channels, μ, detuning of the external variable magnetic field, $B(t)$, from its resonant value B_0, and transverse trap frequency $\omega_\perp$,

$$|g|^2 = \omega_\perp |a_{\rm bg}\mu|\Delta, \quad D_{\rm 1D}(t) = \mu[B(t) - B_0] - \omega_\perp . \quad (10)$$

The effect of the confinement-induced resonance [31] is neglected in Eq. (10), as $a_{\rm bg}$ is much smaller than the transverse size of the trap. The source of the quantum noise in Eq. (9), $\hat{F}(X,t)$, and rate coefficient k_a account for the deactivation in atom-molecule inelastic collisions [25]. Rate coefficients k_a and k_m (for molecule-molecule collisions) are related to their 3D counterparts, $k_{a,m} = (m\omega_\perp/2\pi)k_{a,m}^{(\rm 3D)}$.

Neglecting the collision-induced deactivation, and replacing the atomic-field operator $\hat{\Psi}_a(X,t)$ by c-number mean field $\varphi_0(X,t)$, the substitution

$$\varphi_0(X,t) = -\Phi u \exp\left(-i\int \Omega(t)dt\right),$$

$$\varphi_m(X,t) = -\sqrt{2}\Phi v \exp\left(-2i\int \Omega(t)dt\right),$$

$$t = z/(2\sqrt{2}g\Phi), \quad X = x/(2^{5/4}\sqrt{mg\Phi}), \quad D_{\rm 1D} = \sqrt{2}g\Phi(\alpha - 4) \quad (11)$$

with $\Omega(t) \equiv -D_{\rm 1D}(t)/2 - 2\sqrt{2}g\Phi$, casts Eqs. (8) and (9) precisely in the form of Eqs. (1), which are adopted in nonlinear optics. Necessary normalization of u and v can be provided by the proper choice of the mean-field scaling constant, Φ, in Eqs. (11).

Effects of deactivation and quantum fluctuations neglected in normalized equations (1) can be taken into regard in the framework of the parametric approximation [25], where the X dependence of φ_m is neglected, and the atomic field operator is represented as

$$\hat{\Psi}_a(X,t) = (1/\sqrt{2\pi})\int dp e^{ipx} C(t)[\hat{A}(p,t)\psi_c(p,t) + \hat{A}^\dagger(-p,t)\psi_s(p,t)],$$

$$C(t) = \exp\left(-\frac{1}{2}\int_0^t dt' k_a |\varphi_m(t')|^2\right). \quad (12)$$

Here, c-number functions $\psi_{c,s}(p,t)$ satisfy the time-evolution equations,

$$i\dot{\psi}_{c,s}(p,t) = \left(\frac{p^2}{2m} - \frac{1}{2}D_{\rm 1D}(t)\right)\psi_{c,s}(p,t) + 2g^*\varphi_m(t)\psi_{s,c}^*(p,t). \quad (13)$$

In the present analysis, the initial moment, $t=0$, corresponds to a relatively small detuning. As the initial state is implied to be a stable condensate, Eq. (12) may be considered, at $t=0$, as the Bogoliubov transformation, with operators $\hat{A}(p,0)$ being annihilation operators of the Bogoliubov quasiparticles. In this case, initial conditions for functions $\psi_{c,s}(t)$ are produced by the Bogoliubov transform,

$$\psi_c(p,0) = \left(\frac{d_p + \epsilon_p}{2\epsilon_p}\right)^{1/2}, \quad \psi_s(p,0) = -2\frac{g^*\varphi_m(0)}{d_p + \epsilon_p}\psi_c^*(p,0)$$

(for $p \neq 0$), where $d_p \equiv p^2/(2m) - D_{\rm 1D}(0)/2 - E$, the Bogoliubov excitation energy is $\epsilon_p = \sqrt{d_p^2 - 4|g\varphi_m(0)|^2}$, and E is the chemical potential of the atom-molecule condensate. At zero temperature, one has $\hat{A}(p,0)|{\rm in}\rangle = (2\pi)^{1/2}\varphi_0(0)\delta(p)|{\rm in}\rangle$, where $|{\rm in}\rangle$ is the initial-state vector, and the atomic-condensate mean field $\varphi_0(t)$ is expressed in terms of solutions to Eq. (13), which satisfy initial conditions $\psi_c(0,0) = 1$, $\psi_s(0,0) = 0$, as follows:

$$\varphi_0(t) = \langle {\rm in}|\hat{\Psi}_a(X,t)|{\rm in}\rangle = C(t)[\psi_c(0,t)\varphi_0(0) + \psi_s(0,t)\varphi_0^*(0)].$$

Then, the normal and anomalous densities in Eq. (8) become X independent, as shown in Ref. [25],

$$\langle \hat{\Psi}_a^\dagger(X,t)\hat{\Psi}_a(X,t)\rangle = |\varphi_0(t)|^2 + \frac{1}{2\pi}\int_{-\infty}^{+\infty} dp n_s(p,t),$$

$$\langle \hat{\Psi}_a(X,t)\hat{\Psi}_a(X,t)\rangle = \varphi_0^2(t) + \frac{1}{2\pi}\int_{-\infty}^{+\infty} dp m_s(p,t),$$

where the momentum distributions of non-condensate atoms, $n_s(p,t)$ and $m_s(p,t)$, can be expressed in terms of $\psi_{c,s}(p,t)$ [25]. Accordingly, the equation for the molecular mean field, Eq. (8), takes the form of

$$i\dot{\varphi}_m(t) = g\varphi_0^2(t) + \frac{g}{\pi}\int_{p_{\rm min}}^{\infty} dp m_s(p,t) - i\left(\frac{k_a}{2}|\varphi_0(t)|^2 + \frac{k_a}{2\pi}\int_{p_{\rm min}}^{\infty} dp n_s(p,t) + k_m|\varphi_m(t)|^2\right)\varphi_m(t). \quad (14)$$

Unlike the 3D case [25], the 1D problem does not require renormalization, as the integral of m_s is free of the ultraviolet divergence. Nevertheless, it now diverges at zero momentum. This formal infrared divergence is related to phase fluctuations and to the absence of true condensate in the infinite 1D system. However, in the present work we actually consider coordinate-dependent solitons, while the divergence is a consequence of the neglect of the coordinate dependence in the parametric approximation. A more careful analysis of the inhomogeneous case yields an asymptotic estimate, $m_s(p,t) \sim p^2$ for $p \ll p_{\rm min} = \sqrt{mg\Phi}$, where the characteristic momentum $p_{\rm min}$ is inversely proportional to the soliton's size $(1/\sqrt{mg\Phi})$. Thus, $p_{\rm min}$ may be naturally chosen as the lower-integration limit in Eq. (14). The resultant value of the integral features a weak dependence on the lower limit, as the divergence is logarithmic.

The characteristic kinetic energy of the atoms, both in the condensate and not belonging to it, can be expressed in terms of the characteristic momentum as $p_{\rm min}^2/(2m)$. The system may be considered as effectively one dimensional if this energy is much smaller than the transverse excitation energy, $\omega_\perp$, i.e., $\omega_\perp^2 \gg n a_{\rm bg}\mu\Delta/m$, where the total initial density of atoms, $n = m\omega_\perp(|\varphi_0(0)|^2 + 2|\varphi_m(0)|^2)/(2\pi)$, is proportional to

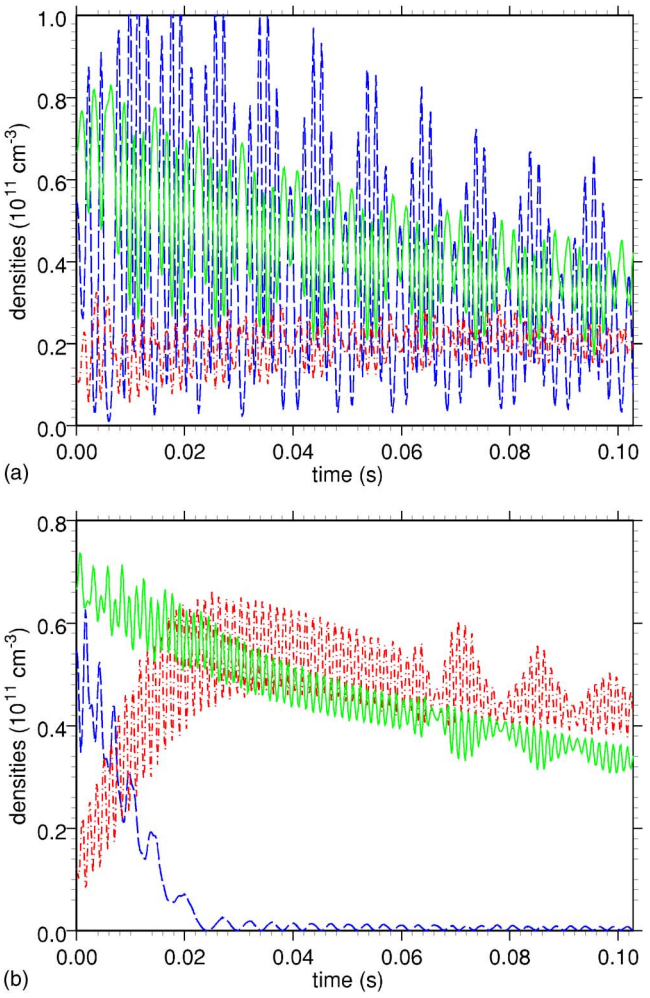

FIG. 6. (Color online) Densities of the molecular and atomic fractions in the condensate (solid and dashed lines), and of noncondensate atoms (dotted-dashed lines), calculated with $\Delta\alpha=1$ for $L=3$ (a) and $L=2$ (b), see Eq. (15).

Manley-Rowe invariant (4), in terms of Eqs. (1).

Further calculations involve a numerical solution of Eqs. (13) on a grid of values of p, combined with Eq. (14). Figure 6 presents the results for the 853 G Feshbach resonance in the condensate of ^{23}Na atoms, with $\Delta=0.01$ G, $a_{\rm bg}=3.4$ nm, and $\mu=3.65\mu_B$ (see Ref. [25]), with $n=2\times10^{11}$ cm^3/s and $\omega_\perp=1\times2\pi$ KHz. The deactivation rate coefficients, $k_a=5.5\times10^{-11}$ cm^3/s and $k_m=5.1\times10^{-11}$ cm^3/s, were taken from Ref. [32]. The detuning $D_{1\rm D}$ is defined as per Eq. (11), with the harmonically modulated mismatch parameter,

$$\alpha=\alpha_0+\Delta\alpha\cos(2\pi z/L), \tag{15}$$

cf. the modulation map in the optical model given by Eq. (3) [recall that z is, in the present contexts, defined in terms of t as per Eqs. (11)]. The choice of the scaling factor in Eqs. (11) which corresponds to the Karamzin-Sukhorukov soliton, see Eqs. (2), is $\Phi=\sqrt{8\pi n/(27m\omega_\perp)}$. The value of $\alpha_0=0.992$ is chosen so as to make the initial molecular fraction equal to one-half the total population, as at the center of the Karamzin-Sukhorukov soliton.

Figure 6(a) demonstrates that, for large modulation periods in Eq. (15), the noncondensate fraction remains below the level of 10%, and the lifetime due to the deactivation is large enough to allow experimental observation of the soliton dynamics described in the preceding sections, in terms of the optical medium, in the hybrid atom-molecule BEC too. The densities demonstrate fast oscillations with the period of the mismatch modulation (about $L\times0.67$ ms under conditions of Fig. 6), as well as slower atom-molecule Rabi oscillations (see Ref. [14]).

However, Fig. 6(b) demonstrates that the noncondensate fraction of the atomic population acquires substantial gain for smaller modulation periods. Therefore, the mean-field approach may not be applicable in this region for the description of the atom-molecular quantum gas, and new instability mechanisms can be expected.

V. CONCLUSIONS

In this work, we have proposed a model of the second-harmonic-generating ($\chi^{(2)}$) system with the mismatch parameter subjected to the periodic modulation ("mismatch management," MM). The system may be implemented in two altogether different physical contexts: the copropagation of the FF (fundamental-frequency) and SH (second-harmonic) waves in a planar optical waveguide, and atomic-molecular mixtures in the BEC (in the latter setting, the atomic and molecular mean fields play the roles of the FF and SH components, respectively). The most physically relevant approach to the realization of the MM in these media are, respectively, a long-period supermodulation imposed on top of the quasi-phase-matching periodic arrangement of ferroelectric domains in the $\chi^{(2)}$ optical waveguide, such as $LiNbO_3$, and the Feshbach resonance tuned by a modulated magnetic field in the atomic-molecular BEC. Accordingly, the natural form of the periodic modulation is piecewise constant in the former case, and harmonic in the latter one.

The main issue considered in the framework of the mean-field approach was identification of the stability region for the mismatch-managed spatial solitons in the plane of two control parameters, $\Delta\alpha$ and L (the MM amplitude and period). In particular, a notable feature of the stability area is the existence of an instability enclave embedded in it. Also investigated was the robustness of the solitons against variation of the shape of the input beam, and reduction of its power. It was found that the stability of the established regime virtually does not depend on the particular shape of the input, as well as on distribution of the total power (Manley-Rowe invariant) between the FF and SH component in the input. On the other hand, reduction of the initial peak power by a factor of $W<1$ reveals the existence of a threshold, $W_{\rm cr}\approx0.72$, below which the initial pulse decays.

In the model of the atomic-molecular BEC, we have demonstrated that the time-evolution equations for the mean fields are tantamount to the spatial-evolution equations in the optical model. Beyond the limits of the mean-field approximation, important issues in the context of BEC are stability of the condensate against generation of fluctuational (noncondensate) components in the degenerate quantum gas, and

losses due to inelastic collisions. These effects were analyzed within the parametric approximation. Numerical calculations have demonstrated that, quite naturally, the condensate is effectively stable against periodic perturbations introduced by the MM in the low-frequency modulation format, and unstable in the high-frequency regime.

ACKNOWLEDGMENT

This work was supported, in a part, by the Israel Science Foundation through a Center-of-Excellence Grant No. 8006/03.

[1] Yu. S. Kivshar and G. P. Agrawal, *Optical Solitons: From Fibers to Photonic Crystals* (Academic, San Diego, 2003).
[2] K. E. Strecker, G. B. Partridge, A. G. Truscott, and R. G. Hulet, New J. Phys. **5**, 73 (2003); F. Kh. Abdullaev, A. Gammal, A. M. Kamchatnov, and L. Tomio, Int. J. Mod. Phys. B **19**, 3415 (2005); O. Morsch and M. Oberthaler, Rev. Mod. Phys. **78**, 179 (2006).
[3] S. K. Turitsyn, E. G. Shapiro, S. B. Medvedev, M. P. Fedoruk, and V. K. Mezentsev, C. R. Phys. **4**, 145 (2003).
[4] B. A. Malomed, *Soliton Management in Periodic Systems* (Springer, New York, 2006).
[5] P. G. Kevrekidis, G. Theocharis, D. J. Frantzeskakis, and B. A. Malomed, Phys. Rev. Lett. **90**, 230401 (2003).
[6] F. Kh. Abdullaev, J. G. Caputo, R. A. Kraenkel, and B. A. Malomed, Phys. Rev. A **67**, 013605 (2003); H. Saito and M. Ueda, Phys. Rev. Lett. **90**, 040403 (2003).
[7] R. Driben and B. A. Malomed, Opt. Commun. **185**, 439 (2000); R. Driben, B. A. Malomed, and P. L. Chu, J. Opt. Soc. Am. B **219**, 143 (2003).
[8] R. Driben, B. A. Malomed, and P. L. Chu, Opt. Commun. **245**, 227 (2005).
[9] R. Driben and B. A. Malomed, Opt. Commun. **197**, 481 (2001).
[10] R. Driben and B. A. Malomed, Opt. Commun. **271**, 228 (2007).
[11] C. Etrich, F. Lederer, B. A. Malomed, T. Peschel, and U. Peschel, in *Progress in Optics*, edited by E. Wolf (North-Holland, Amsterdam, 2000), Vol. 41, p. 483; A. V. Buryak, P. Di Trapani, D. V. Skryabin, and S. Trillo, Phys. Rep. **370**, 63 (2002).
[12] V. Steblina, Yu. S. Kivshar, M. Lisak, and B. A. Malomed, Opt. Commun. **118**, 345 (1995).
[13] P. Di Trapani, D. Caironi, G. Valiulis, A. Dubietis, R. Danielius, and A. Piskarskas, Phys. Rev. Lett. **81**, 570 (1998).
[14] E. Timmermans, P. Tommasini, M. Hussein, and A. Kerman, Phys. Rep. **315**, 199 (1999).
[15] R. A. Duine and H. T. C. Stoof, Phys. Rep. **396**, 115 (2004).
[16] T. Koehler, K. Goral, and P. S. Julienne, Rev. Mod. Phys. **78**, 1311 (2006).
[17] P. D. Drummond, K. V. Kheruntsyan, and H. He, Phys. Rev. Lett. **81**, 3055 (1998).
[18] L. Torner, IEEE Photonics Technol. Lett. **11**, 1268 (1999).
[19] L. Torner, S. Carrasco, J. P. Torres, L. C. Crasovan, and D. Mihalache, Opt. Commun. **199**, 277 (2001).
[20] L. E. Myers, R. C. Eckardt, M. M. Fejer, R. L. Byer, W. R. Bosenberg, and J. W. Pierce, J. Opt. Soc. Am. B **12**, 2102 (1995).
[21] M. Trippenbach, M. Matuszewski, and B. A. Malomed, Europhys. Lett. **70**, 8 (2005); M. Matuszewski, E. Infeld, B. A. Malomed, and M. Trippenbach, Phys. Rev. Lett. **95**, 050403 (2005).
[22] B. A. Malomed, D. Mihalache, F. Wise, and L. Torner, J. Opt. B: Quantum Semiclassical Opt. **7**, R53 (2005).
[23] Y. Lai and H. A. Haus, Phys. Rev. A **40**, 854 (1989); A. G. Shnirman, B. A. Malomed, and E. Ben-Jacob, *ibid.* **50**, 3453–3463 (1994).
[24] V. A. Yurovsky, A. Ben-Reuven, and M. Olshanii, Phys. Rev. Lett. **96**, 163201 (2006).
[25] V. A. Yurovsky and A. Ben-Reuven, Phys. Rev. A **67**, 043611 (2003).
[26] H. A. Haus and C. X. Yu, J. Opt. Soc. Am. B **17**, 618 (2000).
[27] L. Torner, D. Mazilu, and D. Mihalache, Phys. Rev. Lett. **77**, 2455 (1996); C. Etrich, U. Peschel, F. Lederer, and B. A. Malomed, Phys. Rev. E **55**, 6155 (1997); D. Mihalache, D. Mazilu, L.-C. Crasovan and L. Torner, Opt. Commun. **137**, 113 (1997); D. Mihalache, D. Mazilu, B. A. Malomed, and L. Torner, *ibid.* **169**, 341 (1999); D. Mihalache, D. Mazilu, L.-C. Crasovan, L. Torner, B. A. Malomed, and F. Lederer, Phys. Rev. E **62**, 7340 (2000).
[28] Y. N. Karamzin and A. P. Sukhorukov, Zh. Eksp. Teor. Fiz. Pis'ma Red. **20**, 730 (1974) [JETP Lett. **20**, 338 (1975)].
[29] H. Sakaguchi and B. A. Malomed, Phys. Rev. E **70**, 066613 (2004).
[30] V. A. Yurovsky, Phys. Rev. A **71**, 012709 (2005).
[31] M. Olshanii, Phys. Rev. Lett. **81**, 938 (1998).
[32] T. Mukaiyama, J. R. Abo-Shaeer, K. Xu, J. K. Chin, and W. Ketterle, Phys. Rev. Lett. **92**, 180402 (2004).